Supplement of:

Earthquake Catalog and Continuous Waveforms from a Two-Week Distributed Acoustic Sensing experiment on Kefalonia Island, Greece.

5

Gian Maria Bocchini[1], Emanuele Bozzi[2], Marco P. Roth[1], Sonja Gaviano[3], Giulio Pascucci[2], Francesco Grigoli[2], Ettore Biondi[4], Efthimios Sokos[5], Rebecca M. Harrington[1]

[1]Institute of Geosciences, Ruhr University Bochum, Bochum, Germany.
[2]Department of Earth Sciences, University of Pisa, Pisa, Italy
10 [3]Seismix srl, Palermo, Italy
[4]Stanford University, Geophysics Department, 397 Panama Mall, Stanford, CA 94305, USA
[5]Department of Geology, Seismological Laboratory, University of Patras, Patras, Greece

Correspondence to: Gian Maria Bocchini (gian.bocchini@rub.de)

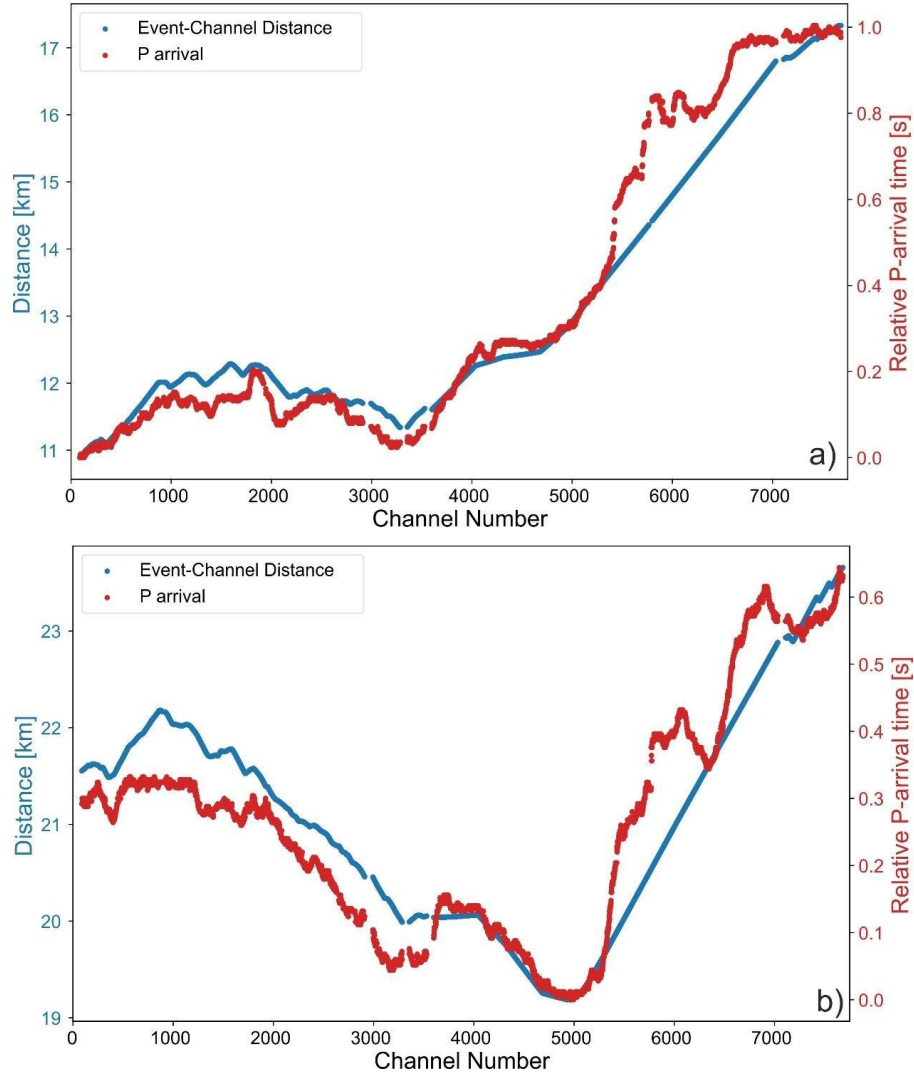15

Content:

Figure S1-S13

Table S1

Figure S1. Event-channel distances and relative P arrivals. P arrivals are obtained with PhaseNet-DAS (Zhu et al., 2023) and are shown with respect to the earliest P-arrival on the fiber. Epicentral earthquake locations are from the reviewed National Observatory of Athens catalog. a) earthquake on 05 August 2024 at 07:20:21.51, lat: 38.4077, lon: 20.4533, NOA event-id = noa2024phcwq. b) earthquake on 25/08/2024 at 17:55:31.61, lat: 38.2791, lon: 20.4776, NOA event-id = noa2024qsmcp.
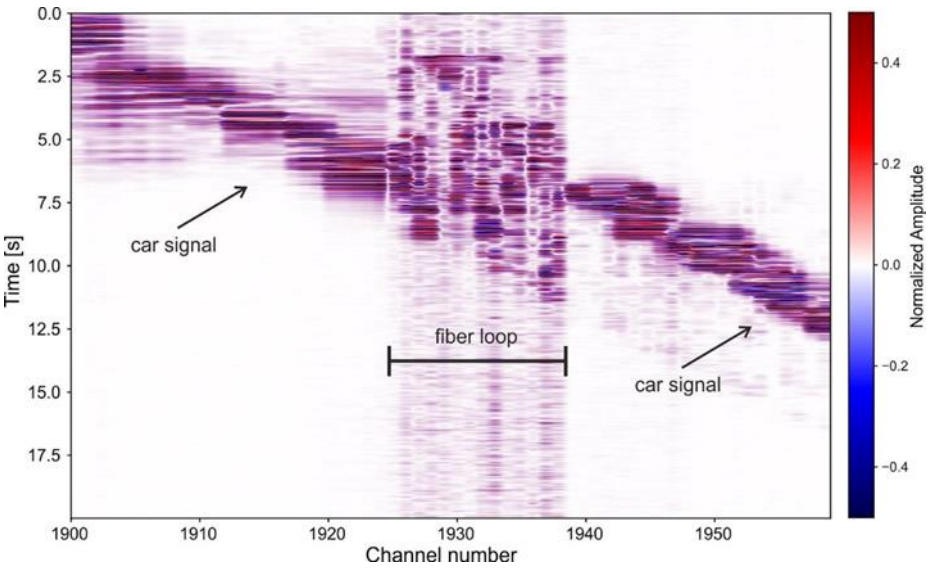
30

Figure S2. Car passing above a fiber loop identified between channels 1925-1938. Traces are bandpass filtered 5-20 Hz and normalized.
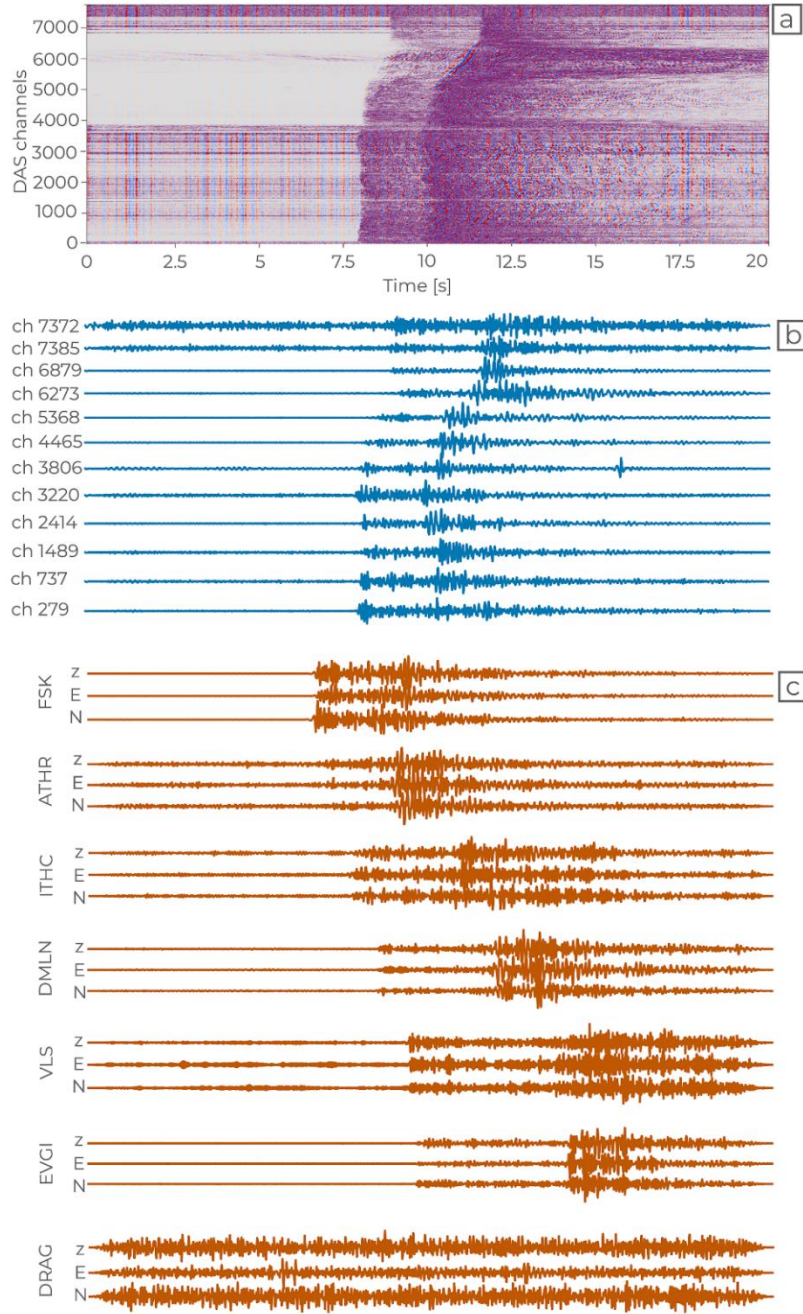
35

Figure S3: Earthquake waveforms from DAS (blue) and seismic stations (dark orange). a) DAS record of the earthquake along the entire optical fiber. b) Waveforms at the median DAS channel from each of the 12 segments we used for earthquake location (Fig. 1). c) Waveforms at seismic stations used for earthquake location. The event is reported in the revised NOA catalog with id = noa2024pgtws and a M_L 1.3 (event kef0884 in the catalog from this study). Waveforms bandpass filtered 5-30 Hz and normalized.
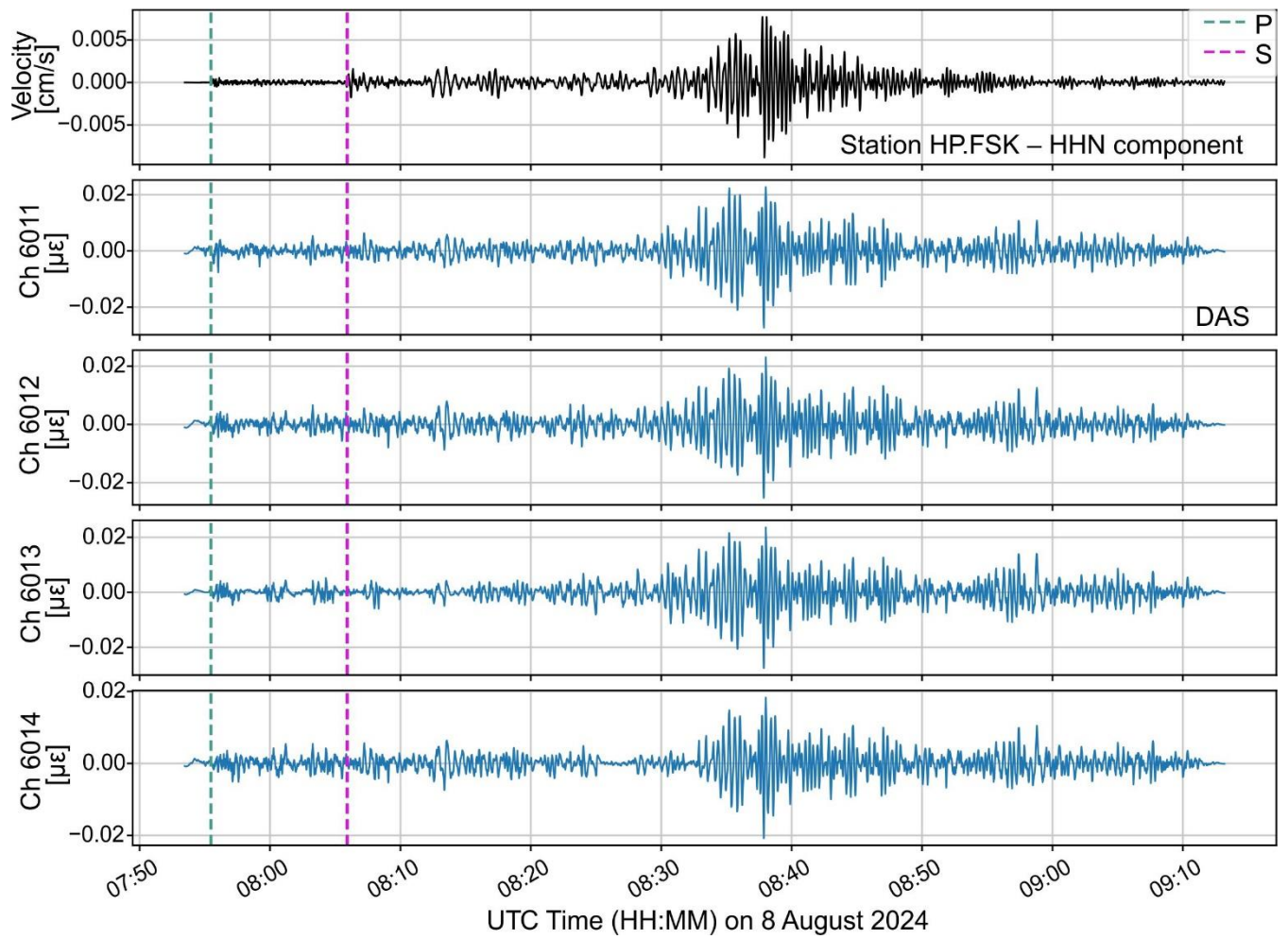
Figure S4: Example of teleseismic event recorded along the offshore part of optical fiber. The black trace shows the teleseismic event at station FSK (Fig. 1) while the blue traces show the teleseismic events recorded by the DAS interrogator along the offshore channels (channels 6011-6014). Traces are bandpass filtered 0.01-1 Hz.
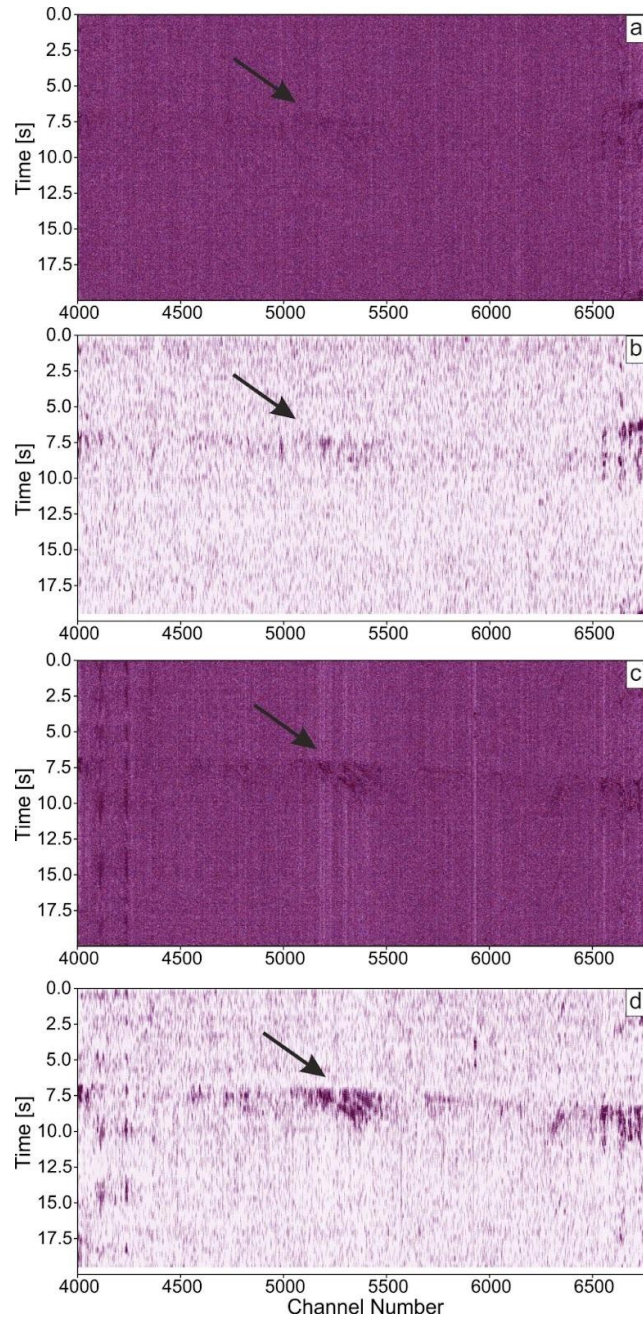
45

Figure S5: Examples of low-SNR events before and after denoising with the spectral over-subtraction method (Pascucci et al., 2025). a) event kef1800 before denoising b) event kef1800 after denoising c) event kef3840 before denoising, d) event kef3840 after denoising. Traces are bandpass filtered 5-20 Hz and normalized. In all cases, a clear SNR improvement is achieved, allowing better identification of weak events. Note the larger signal amplitudes between channels 5000-5500 (indicated by the arrow in the panels).
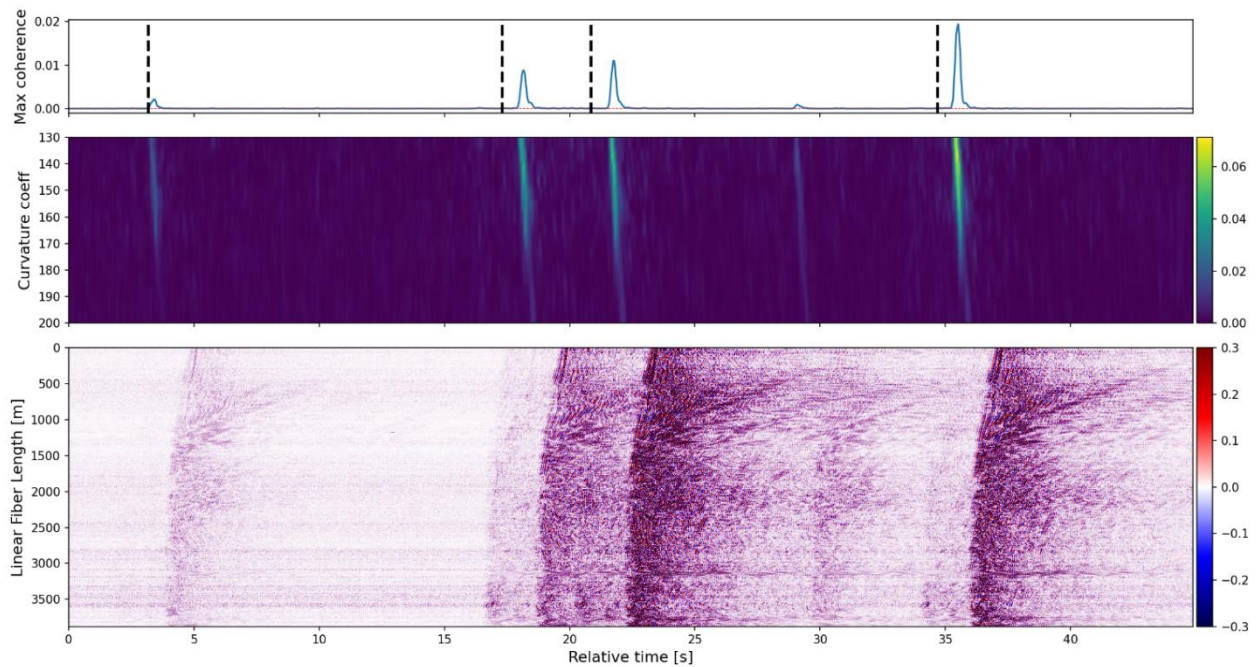
50

6

Figure S6. Example of missed events at ~30 seconds. (top panel) Coherence time series over a 45-s window, showing four detections. Vertical dashed black lines mark the earthquake detection times. (middle panel) Semblance matrix, where the maxima highlight the events detected by HECTOR. (c) Real DAS data recorded during the Kefalonia experiment. The y-axis shows channels ranging from 4000 (bottom) to 5900 (top). The x-axis origin corresponds to 2024-08-08 23:34:11. Traces are processed as described in the main text (section 3).
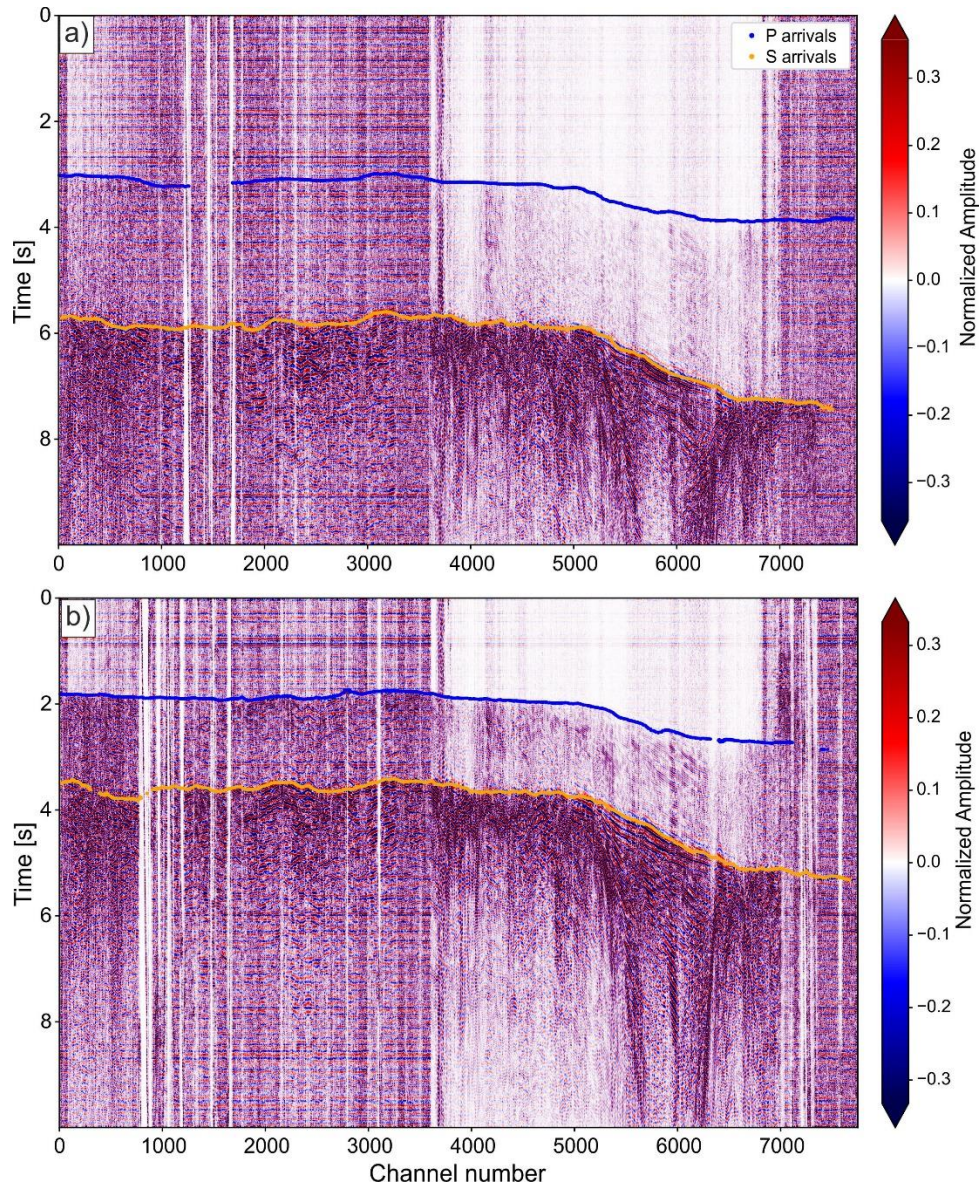
Figure S7. Example PhaseNet-DAS predicted arrival times for events in the Kefalonia dataset. (a) Event kef0131 with M_L 1.0. (b) Event kef0140 with M_L 0.7. Traces are bandpass filtered 5-20 Hz and normalized. Note that the data processing applied in this figure is not the same applied for picking with PhaseNet-DAS (see Section 4).
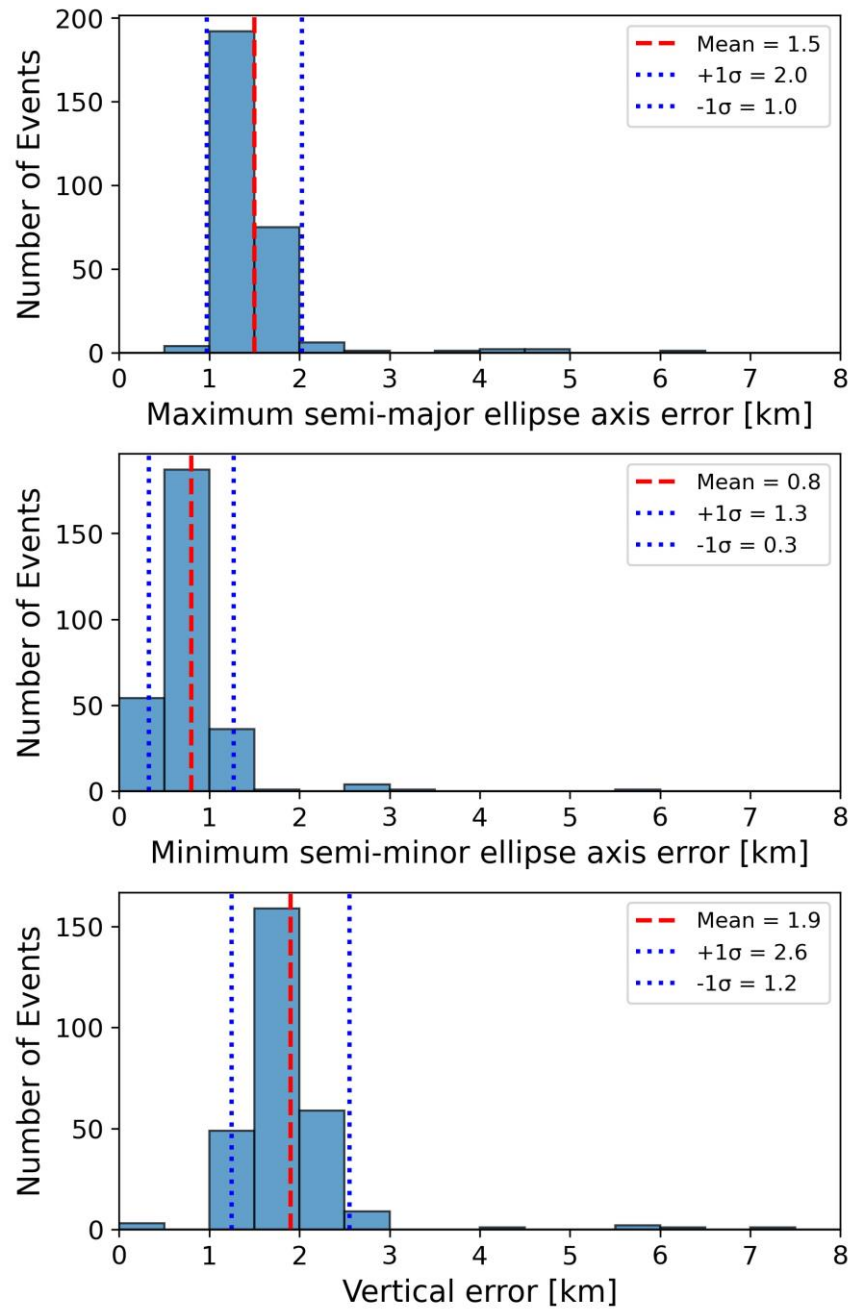
95

Figure S8. Histograms of location errors for the 284 earthquakes located using DAS and seismic station data.
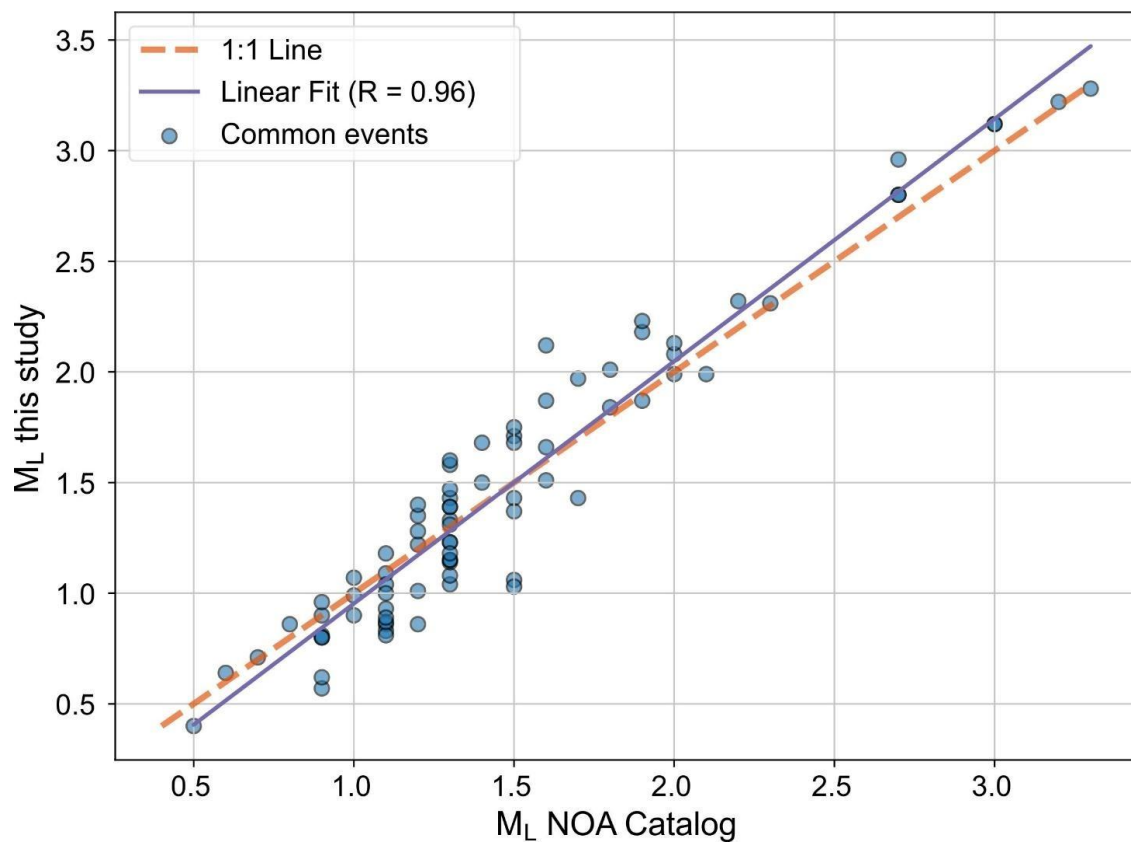
Figure S9. Comparison of local magnitudes (M_L) obtained from the National Observatory of Athens with those obtained in this study from common events in both catalogs.
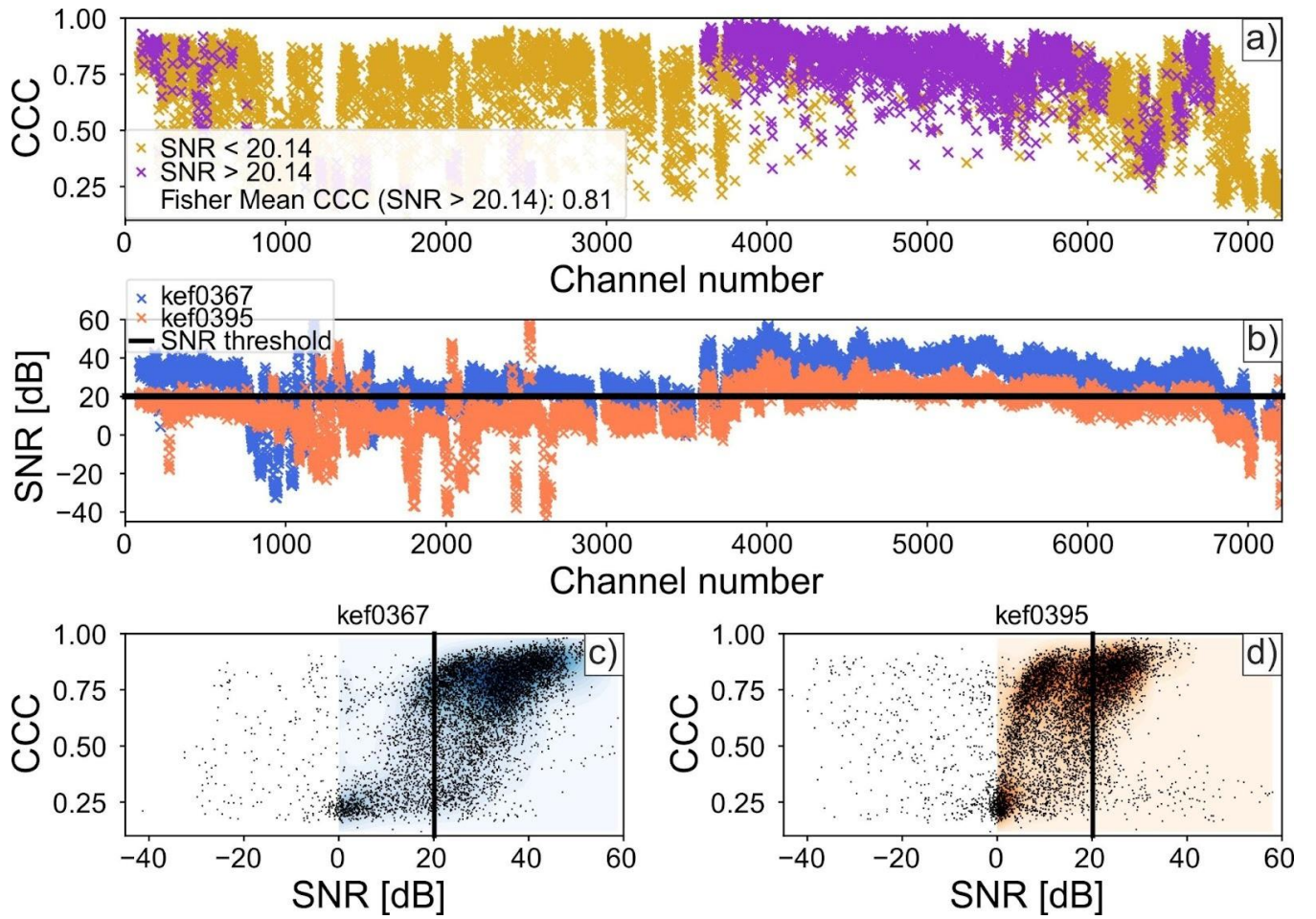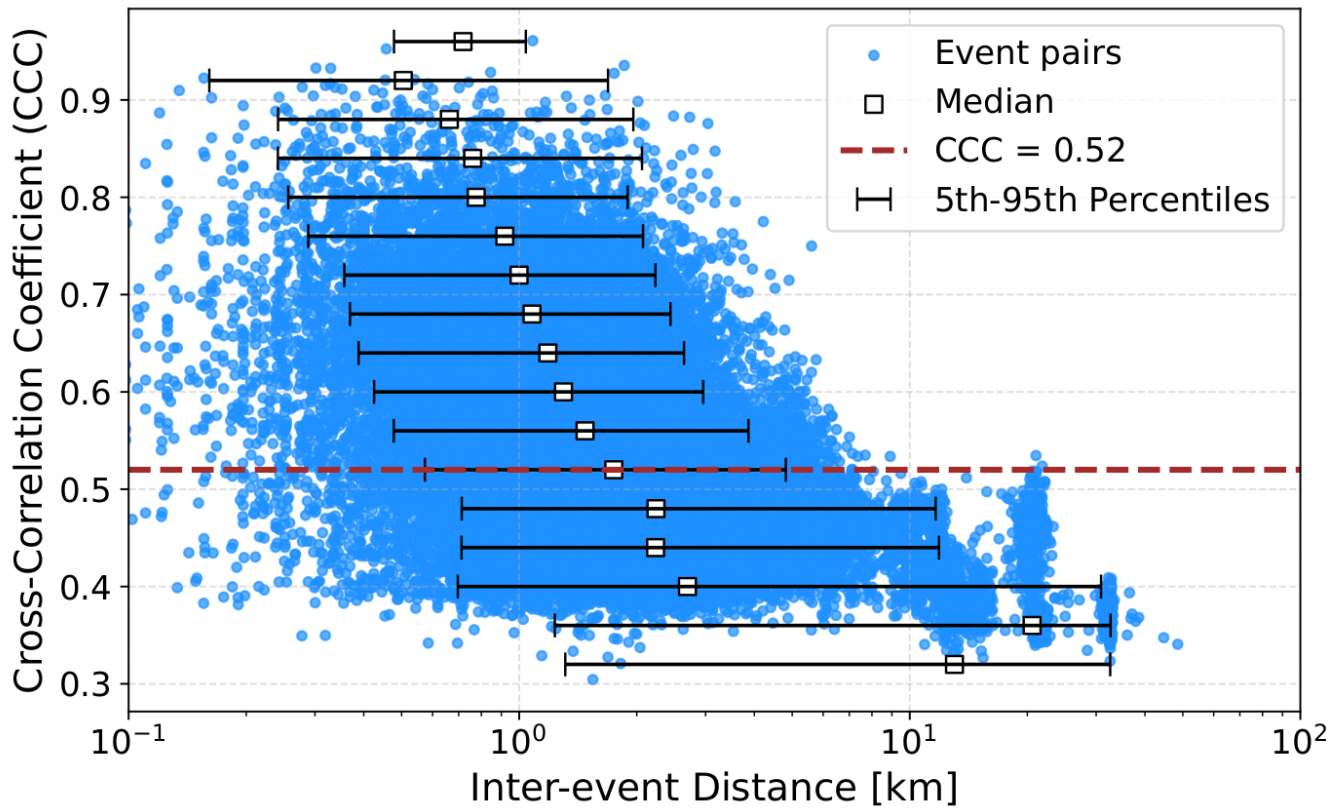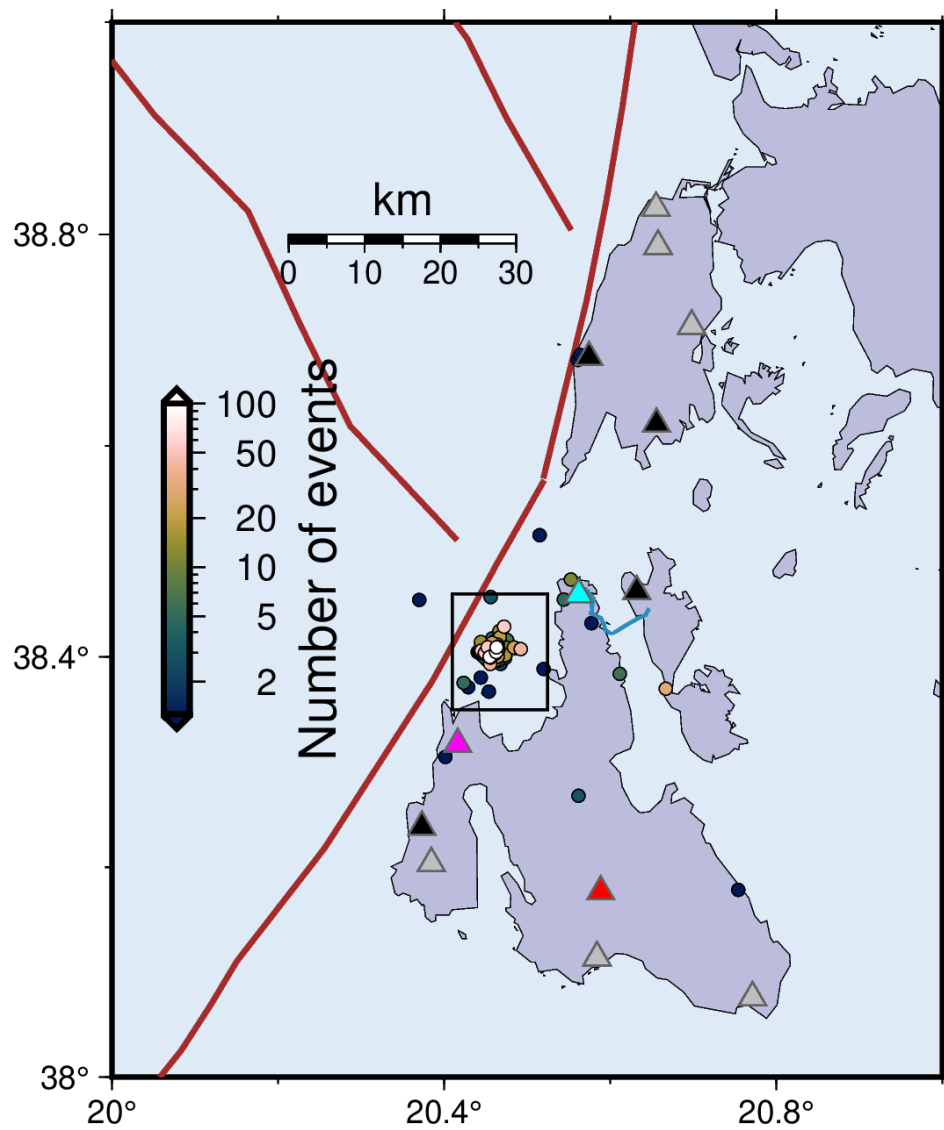
Figure S10. Waveform Cross-Correlation Coefficient (CCC) analysis for event pair kef0367 (M$_L$ 1.7) and kef0395 (M$_L$ 1.0). (a) CCC of individual DAS traces along the entire cable length (identified cable loops are excluded). (a) Purple and gold symbols are CCC values above and below a SNR threshold calculated from the smaller amplitude event in the pair (see text and description in panel b of this figure). (b) Signal-to-noise ratio (SNR) of each event in the pair. SNR (in dB) is calculated as the ratio between the root-mean-square of the signal in 4-second windows starting 0.5 s after the detection time and noise windows of the same length starting 5 s before the detection time (refer to Fig. 3a for SNR windows). The thick horizontal black line marks the minimum SNR threshold required for the CCC calculation, which is defined by the lower-amplitude event. The threshold corresponds to the cutoff of the top 33% of channels with the highest SNR. (c–d) CCC versus SNR for events kef0367 and kef0395. The vertical black line indicates the minimum SNR threshold. Average cross-correlation coefficient of the event pair is 0.85, estimated as the Fisher mean of the individual CCC values. Traces are bandpass-filtered 5-20 Hz.
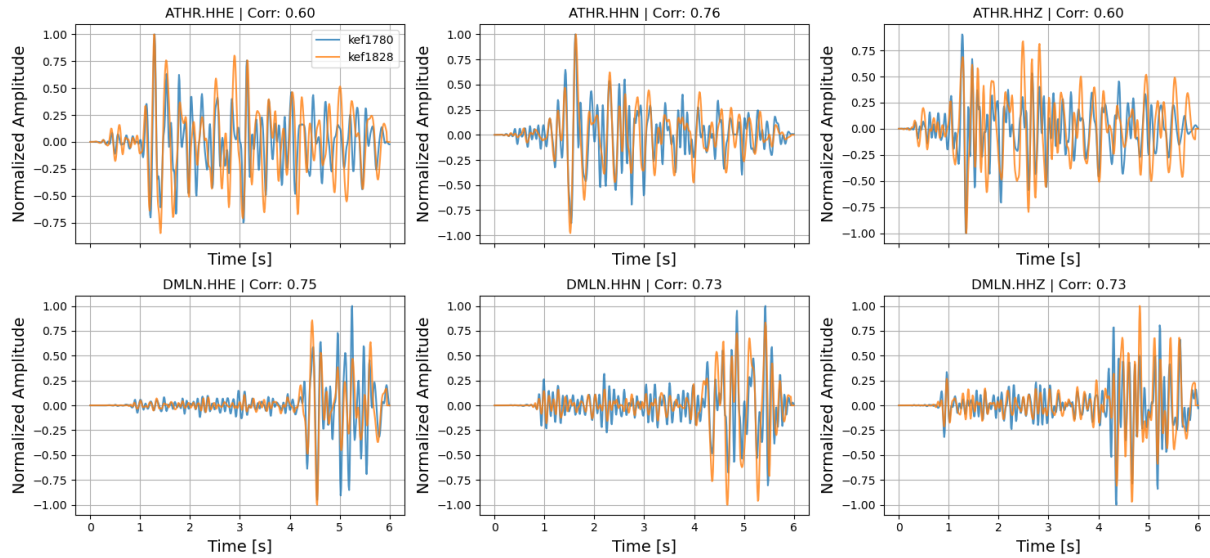
Figure S11. Cross-correlation coefficient (CCC) versus hypocentral interevent distance for all located earthquakes with semi-major ellipse error axis and vertical error < 5 km (284 earthquakes). Median interevent distances, along with the 5th and 95th percentiles, are computed using a CCC bin size of 0.04. For example, the median distance reported at CCC = 0.52 is calculated from values in the range 0.50–0.54. At CCC = 0.52, the median interevent distance is < 2 km.

120   **Figure S12. Event locations in the enhanced seismicity catalog, obtained after waveform cross-correlation between template and target events. Circles mark the template event locations and are color-coded by the number of associated target events.4 Discussion**

Event comparison: kef1780 vs kef1828

125 **Figure S13. Cross-correlation coefficient and waveforms of events kef1780 and kef1828 at seismic stations ATHR and DMLN. Waveforms are bandpass filtered 3-12 Hz and normalized to make the event amplitudes comparable.**

Table S1. 1D Velocity model used for earthquake locations. Slightly modified from Haslinger et al. (1999)

Depth (km)	Vp (km/s)	Vp gradient	Vs (km/s)	Vs gradient
0	3.5	1	1.9	0.48
2	5.5	0.167	2.86	0.12
5	6	0.04	3.23	0.002
10	6.2	0.056	3.24	0.032
15	6.48	0.044	3.4	0.08
20	6.7	0.005	3.8	0.001
30	6.75	0.125	3.81	0.081
40	8	0	4.62	

References in supplement

Haslinger, F., Kissling, E., Ansorge, J., Hatzfeld, D., Papadimitriou, E., Karakostas, V., Makropoulos, K., Kahle, H. G., and Peter, Y.: 3D crustal structure from local earthquake tomography around the Gulf of Arta (Ionian region, NW Greece), Tectonophysics, 304, 201–218, https://doi.org/10.1016/S0040-1951(98)00298-4, 1999.

135   Pascucci, G., Gaviano, S., Pozzoli, A., Grigoli, F: Signal Enhancement of Distributed Acoustic Sensing data using a Spectral Subtraction-based Approach. Seismol. Res. Lett., (in-press)

Zhu, W., Biondi, E., Li, J., Yin, J., Ross, Z. E., and Zhan, Z.: Seismic arrival-time picking on distributed acoustic sensing data using semi-supervised learning, Nat. Commun., 14, 1–11, https://doi.org/10.1038/S41467-023-43355-3, 2023.